THE ASTRONOMICAL JOURNAL VOLUME 83, NUMBER 7 JULY 1978

OBSERVATIONS OF RADIO SOURCES WITH FLAT SPECTRA

FRAZER N. OWEN[a] and RICHARD W. PORCAS[a)c)]
National Radio Astronomy Observatory,[b] Green Bank, West Virginia 24944

STUART L. MUFSON[a]
Astronomy Department, Indiana University, Bloomington, Indiana 47401

THOMAS J. MOFFETT[a]
Department of Physics, Purdue University, West Lafayette, Indiana 47907
Received 10 April 1978

ABSTRACT

Observations made in January 1977 are presented for 237 sources with flat or inverted radio spectra at centimeter wavelengths (α 0,$S \propto \nu^{\alpha}$). Flux densities measured at 90 GHz with the NRAO 11-m telescope are given for all 237 sources. In addition, nearly simultaneous measurements made with the VLA for 104 sources at 1.4, 4.6, 15.1, and 22.2 GHz are presented. Optical *U B V* photometry with the Kitt Peak 2.1-*m* telescope, simultaneous with the millimeter measurements, is also given for 9 of the sources. Forty-one sources were detected above 1 Jy at 90 GHz. The radio spectra of the majority of these sources are flat ($\alpha \sim 0$) over the range 1–100 GHz. Comparison with measurements at 90 GHz made a year earlier shows that variability at this frequency is rarely more than 30% over this time. Optically, the small sample we observed suggests much more rapid variability. One source, 1308+32, varied by 10% over one year at 90 GHz while optically over the same period it varied by a factor of 10 and increased 30% over the four nights it was observed during this program. The spectra and variability properties are consistent with incoherent synchrotron models with radially decreasing relativistic particle densities and/or magnetic field strengths. In this picture the millimeter and centimeter emission is optically thick and comes from a region typically 1 pc. The optical emission arises from optically thin regions much nearer the center of the emitting region.

I. INTRODUCTION

Radio sources with flat ($\alpha \sim 0$, $S \propto \nu^{\alpha}$) or inverted spectra ($\alpha > 0$) at centimeter wavelengths have proven to be some of the most interesting extragalactic objects known. Most of these sources are apparently opaque (optically thick) synchrotron sources. In January 1976, we observed a sample of 38 such sources with the 11-m telescope at 90 GHz (Owen and Mufson 1977; hereafter Paper I). Of these sources about 25% were found to have flat spectra from 5 to 90 GHz, based on the 1972 Green Bank Survey flux densities (Pauliny-Toth *et al.* 1972; Pauliny-Toth and Kellermann 1972) and our 1976 90 GHz measurements. However, sources with opaque radio spectra are known to be often variable and thus simultaneous measurements are really needed to define the spectra. In Paper I a correlation was found between the 90 GHz flux density and the optical magnitude of the identification from the Palomar Sky Survey. This result was somewhat surprising to us since the sky survey plates were taken generally in the early 1950's and the optical counterparts of these sources were known to be variable on timescales of years.

In order to study the radio and optical properties of this class of sources, we made simultaneous or nearly simultaneous observations of a large sample of them at optical, infrared, and radio wavelengths. The infrared results along with the related optical and radio data are discussed elsewhere (O'Dell *et al.* 1978). In this paper we describe the radio and optical observations made at Kitt Peak and the VLA between 14 January and 9 February 1977.

II. OBSERVATIONS AND RESULTS

a) The Source Sample

As in Paper I, objects included in the sample for observation at 90 GHz were those having a flat or rising spectral index in the neighborhood of 5 GHz. The prime sample observed at 90 GHz consisted of 161 objects with the following properties: (a) The spectral index $\alpha(S \propto \nu^{\alpha})$ in the neighborhood of 5 GHz was greater than -0.2. The spectral index $\alpha(0.318,5)$, in the notation of Paper I, was the one on which the classification was ordinarily made. In some cases, the spectral index used was defined between 5 GHz and either 0.966, 2.695, or 10 GHz.

[a]Visiting astronomer at Kitt Peak National Observatory, which is operated by the Association of Universities for Research in Astronomy, Inc., under contract with the National Science Foundation.

[b]The NRAO is operated by Associated Universities, Inc., under contract with the National Science Foundation.

[c]Present address: Max-Planck-Institut für Radioastronomie, Auf dem Hügel 69, D-5300 Bonn 1, W. Germany.

 0004-6256/78/8307-0685$00.90

However, for a few sources the 5 GHz density was unknown; for these objects, the spectral index was estimated from flux densities measured at two other of the above frequencies. (b) The sources were required to have a flux at 5 GHz, $S_5 \geq 0.6$ Jy. For some sources this flux density was interpolated from the spectral index and a flux density at an adjacent frequency. (c) The sources had a declination in the range $-4° \leq \delta \leq 90°$, and a right ascension in the range 0 hours $\leq \alpha \leq$ 16 hours. The restriction on the right ascension was imposed because we planned simultaneous observations of the brightest objects in the 90 GHz survey at optical and infrared wavelengths. Our prime source list was drawn mainly from the Green Bank 5 GHz survey (Pauliny-Toth *et al.* 1972, Pauliny-Toth and Kellermann 1972, Pauliny-Toth *et al.* 1978). Additional sources were included from Brandie and Bridle (1974), Porcas (1975), and Wall *et al.* (1971). As time permitted, we also observed objects from a second priority list in which either condition (2) or (3) was relaxed. In total, 237 sources were observed at 90 GHz.

Our prime source list represents an attempt to construct a complete sample based on well-defined selection criteria. However, the spectral index was not always estimated between the same two frequencies. In addition, the flux densities used to calculate the spectral index were usually obtained at different epochs. Since sources with flat spectra are known to be time variable, it can be seen that the spectral index is not always a source parameter which is well determined. In addition to this problem in determining the spectral index, the population of sources with $S_5 \geq 0.6$ Jy also fluctuates with time. Consequently, our prime source list can be considered only approximately complete at the time of our observations.

From the results of our survey at 90 GHz, a subsample of 41 objects with $S_{90} \geq 1.0$ Jy was selected for simultaneous observations at optical and infrared wavelengths. Poor weather, however, resulted in usable data for only 9 objects. For later observations with the VLA, two subsamples of objects were chosen: (1) the 38 sources discussed in Paper I, and (2) the 41 sources with $S_{90} \geq$ 1.0 Jy. As time permitted, other objects were added to the source list, and a total of 104 objects was observed with the VLA.

b) *Radiometry at 90 GHz*

The 90 GHz observations were made with the NRAO 36-ft (11-m) telescope at Kitt Peak during the period 14–19th January 1977. At this frequency the telescope beamwidth (FWHM) is approximately 75 arcsec. The radiometer consisted of a cooled mixer receiver with two orthogonal linear polarization channels. Both channels accepted two sidebands, each of 500 MHz, and centered on frequencies of 85.5 and 94.5 GHz. Beam-switching observations were made by nutating the subreflector at a rate of 5 Hz to product two beams separated in azimuth by 225 arcsec. The switched outputs of the two channels were combined together, logged by the on-line computer and integrated for a period of 30 s.

TABLE I. Center frequencies, bandwidths and feed polarizations for the VLA observations.

Band	Center frequency	Bandwidth	Polarization
L	1.379 GHz	12.5 MHz	orthogonal linear
C	4.585 GHz	50 MHz	opposite circular
U	15.064 GHz	50 MHz	opposite circular
K	22.185 GHz	50 MHz	opposite circular

Observations of the program sources were made within three hours of meridian transit, and consisted of 21 consecutive integrations, alternatively positioning the main and reference beams on the source postion. At the conclusion of an observation the average on-minus-off source antenna temperature and its standard error were computed from a knowledge of the receiver gain fluctuations and the atmospheric attenuation. These were determined every 4 h by measuring the variation of system temperature due to atmospheric emission as a function of elevation angle, and by injecting an 8.4 K noise signal into the front of the receiver.

The overall system gain and telescope pointing equation were monitored every hour by making pointing observations of strong calibration sources. These sources were 3C 84, DR 21, Venus, Saturn and Jupiter, for which peak flux densities appropriate to this instrument were available (Ulich, private communication). The flux density scale is based on an assumed value of 16.9 Jy for DR 21 at 90 GHz. The gain factor derived in this manner (~110 Jy/K) was then applied to the measured antenna temperatures. A small (4%) increase was made for the program sources as a statistical correction for pointing errors. The noise error for a single observation was typically 0.15 Jy.

c) *Radiometry at Centimeter Wavelengths*

These observations were made during the periods 27–31 January and 8–9 February 1977, with the Very Large Array (VLA) telescope, currently under construction near Socorro, New Mexico (see, e.g., Heeschen 1975). For this project we used four of the 25-m antennas, which were stationed along the south-west arm of the array (azimuth 236°).

The antennas were equipped with single side-band receivers for operation at L, C, KU ("U") and K radio frequency bands. A Cassegrain system is used which allows the feed for a particular frequency band to be selected by rotation of the asymmetric subreflector. For this experiment the receivers each had two channels for opposite senses of polarization. The center frequencies, bandwidths and feed polarizations used are given in Table I.

The main amplification stage of the receivers consists of a low-noise 5 GHz cooled parametric amplifier, which is connected directly to the feed for C band observations.

TABLE II. Baselines for which the data were analyzed.

Antenna pair	Baseline length	Bands
1–2	4739 m	*L*
1–4	1106 m	*C, U, K*
2–4	3633 m	*K*
3–4	1500 m	*C, U, K*

For L band observations it is preceded by a parametric up-converter, while at U and K bands there are cooled mixers ahead of the paramp. Further details of the antennas and front-end system are described in the "VLA User Manual" (1977).

During the observation of a source the I.F. signals from the receivers of each antenna pair were correlated, producing amplitudes and phases every 10 s for both polarizations for each baseline. These were then used off-line to form 1 min vector averages for each correlator. Arithmetic averages of these 1 min samples were then formed where appropriate to reduce errors arising from uncertainties in the signal phase. In all cases the signal-to-noise ratio was high enough for the statistical bias associated with arithmetic averaging to be $\lesssim 1\%$.

Sources were generally observed within 3 h of transit. Most observations consisted of cycling through the 4 frequency bands in the sequence L, U, C, K, with observing times of 2, 5, 2, 5 min, respectively. Some of the later observations were made in different sequences with less optimistic mnemonics. Program source observations were interleaved with observations of calibration sources every 30 or 40 min to monitor the correlator gains as a function of time and antenna elevation. For this purpose 3C 286 was used as the primary flux density scale calibrator, and a number of strong, mostly compact, sources were used as secondary calibrators (3C 48, 3C 120, 3C 147, DA 267, 3C 279, 3C 345). Flux densities for 3C 286 at the four frequencies were determined from the flux densities and spectra published by Kellermann *et al.* 1969, Kellermann and Pauliny-Toth 1973, and Genzel *et al.* 1976, and an unpublished 31 GHz flux density from Geldzahler (1977, private communication). The values derived at L, C, U, and K bands were 14.6, 7.81, 3.43, and 2.70 Jy, respectively.

Owing to various instrumental malfunctions we did not attempt to reduce data from all baselines at all frequency bands; rather, we selected baselines at each frequency which gave repeatable amplitudes on calibration sources and consistent gain versus elevation curves. The antenna pair, baseline length and bands for which data were analyzed are listed in Table II. Since baselines greater than 1 km were used during this experiment, the flux densities listed apply only to the compact cores of these sources. Any extended structure will have been resolved out by the long baseline. However, only a small fraction of the sources have known extended structures (e.g., 3C 273) and the flat spectra suggest that all of these sources are dominated by a compact component.

At L band the use of linear polarization made it necessary to form the geometric mean of the two polarization correlators to calibrate the antenna gain, since many of the sources exhibit a significant degree of linear polarization. For the other frequencies gain curves were determined separately for the correlators of opposite hands of circular polarization. These curves were then applied to the correlated amplitudes of the program sources. Noise errors for a single correlator and observation at L, C, U and K bands were typically 20, 10, 60 and 150 mJy, respectively. Where appropriate, flux densities from separate correlators and observations were averaged together to form the best estimate of the source flux density.

d) *Results of the Radiometry*

The results of the radio measurements are given in Table III. In column 1 we give the Parkes-type name for each source observed at 90 GHz. The flux densities in Jy obtained with the VLA and their estimated standard errors are given in columns 2, 3, 4, and 5. Column 6 lists the flux densities in Jy and standard errors for the measurement at 90 GHz. In column 7 we give the number of the reference for the source position. The references are given in the footnotes to Table III. In Table IV the positions of 13 sources which were measured in preparation for the program with the Green Bank interferometer at 2.7 GHz are given. Typical errors are $\lesssim 0.5$ arcsec in each coordinate. In Fig. 1 we show the spectra of the 47 sources which were measured at all four VLA frequencies and at 90 GHz.

e) *Optical Photometry*

The optical observations were obtained at Kitt Peak National Observatory using the 2.1-m reflector during the same time interval as the 90 GHz observations were made on the NRAO 11-m telescope. The KPNO computer controlled photometer, with a 1P21 photomultiplier, and the TV acquisition system were used for all observations (KPNO User's Manual 1977).

The observations were transformed to the Johnson *UBV* system by using Landolt's (1973) faint standards. The reductions were done on line by the minicomputer using mean values for extinction and transformation. Later, small nightly zero point corrections were included to produce the final results.

Rather poor weather conditions during the run allowed us to observe only nine of the sources on the program. Most of the observations were obtained differentially using a comparison star in the field. The results of the optical photometry are summarized in Table V. The source name and date of observation are given in columns 1 and 2. The V band magnitude follow in column 3. The $(B - V)$ and $(U - B)$ colors are listed in Columns 4 and 5. The corresponding V (830 THz), B (680 THz), and U (540 THz) flux densities in mJy are given in columns 6, 7, and 8. The number of observations used to

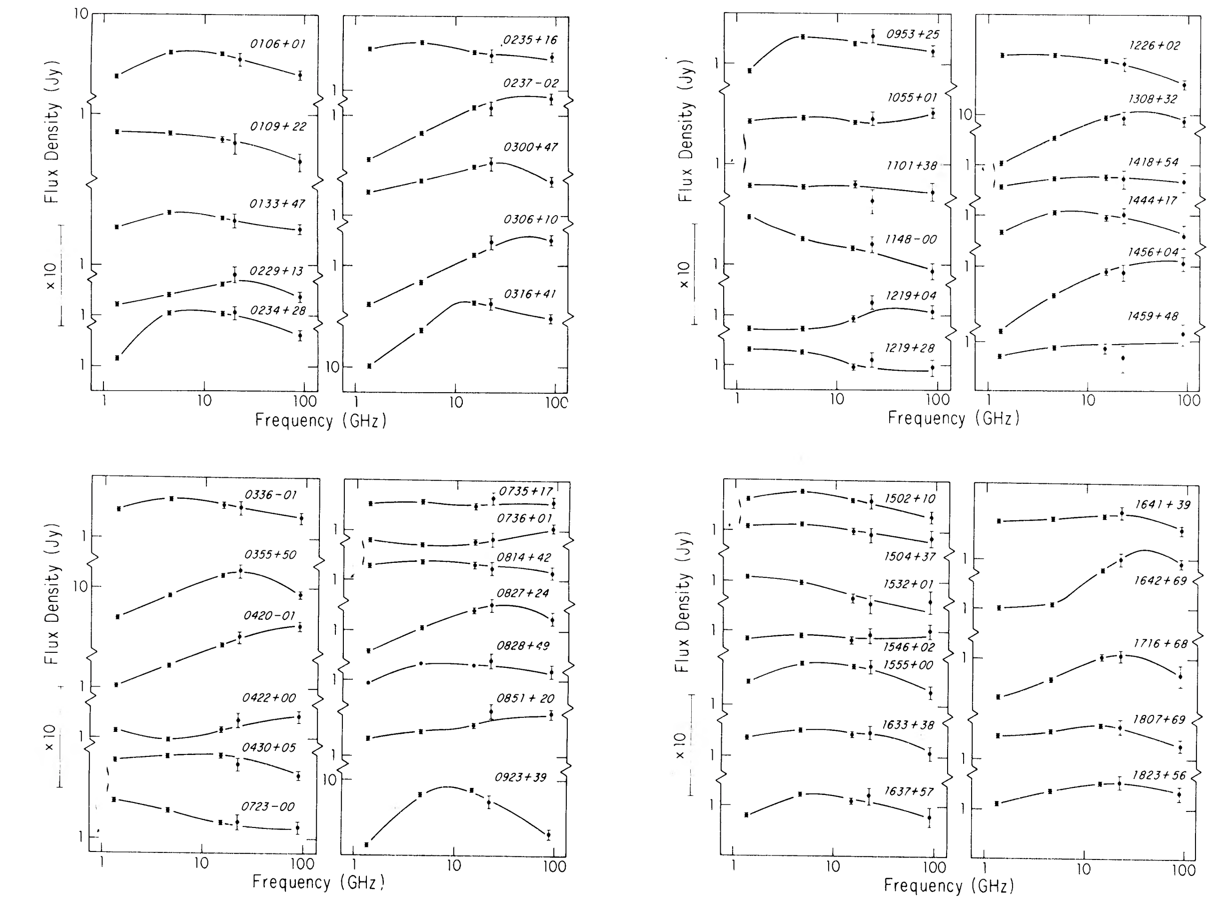

FIG. 1. Radio spectra densities for all sources with measurements at all five frequencies. The log of the flux density in Jy is plotted for each source. The scale is shown by the X10 line ($\Delta \log S = 1$) on the left side of each group of spectra.

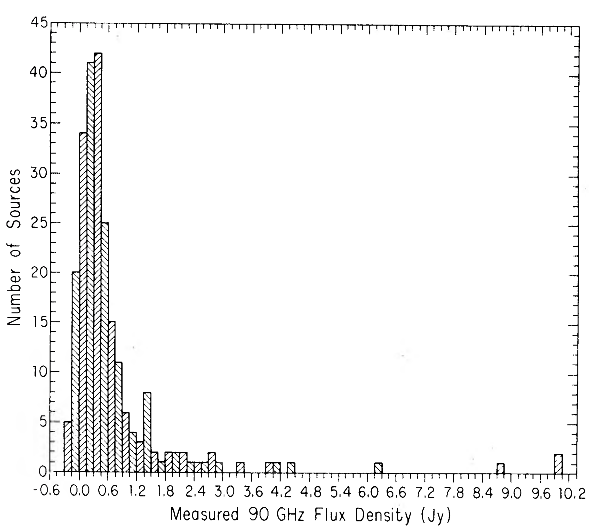

FIG. 2. Histogram of observed flux densities at 90 GHz for all 237 sources.

determine each of these measurements is given in column 9.

Our most interesting optical result concerns 1308 + 32. This source recently had an outburst (Liller 1976) during which it reached a B magnitude of 16.1. O'Dell *et al.* (1977) obtained the following magnitudes and colors for this source in May 1976: $V = 16.20$, $(B - V) = 0.29$, and $(U - B) = -0.49$. As shown in Table V, 1308 + 32 had become about 2 mag brighter by January 1977.

Our results on 0851 + 20 (= OJ287) show that we measured it near its faint limit, as did O'Dell *et al.* (1977). Our measurements of 1219 + 28 are consistent with the V magnitude and $(U - B)$ color of Tapia *et al.* (1976); but our $(B - V)$ color is bluer.

III. PROPERTIES OF THE SAMPLE

a) 90 GHz Flux Density Distribution

In Fig. 2 we show a histogram of the observed 90 GHz flux densities of all 237 sources observed with the 11-m telescope. The noise (standard error) in a single obser-

TABLE III.

SOURCE	1.379 GHZ		4.585 GHZ		15.064 GHZ		22.185 GHZ		90.000 GHZ		
	S±ΔS		S±ΔS		S±ΔS		S±ΔS		S±ΔS		REF
0003+38			0.60	0.03	0.70	0.07			0.60	0.16	1
0007+17									0.33	0.15	6
0012+31									0.30	0.15	6
0013-00									0.39	0.11	1
0022+39									0.21	0.15	1
0024+34									0.18	0.15	1
0035+41									-0.03	0.15	1
0038-02									0.37	0.15	10
0055+30									0.59	0.12	6
0056-00									0.45	0.11	10
0102+48									0.11	0.15	2
0106+01	2.33	0.12	4.04	0.20	3.99	0.21	3.54	0.54	2.48	0.28	9
0108+38			1.26	0.06	0.54	0.07			-0.17	0.15	1
0109+22	0.67	0.04	0.65	0.03	0.56	0.05	0.53	0.13	0.34	0.07	6
0109+35									0.53	0.16	1
0110+49									0.41	0.16	2
0111+02					0.73	0.07			0.78	0.17	11
0112-01									0.33	0.15	1
0119+04			1.04	0.05	0.94	0.08			0.82	0.17	6
0119+11									0.11	0.15	6
0119+24			0.68	0.04	0.50	0.06			0.22	0.15	6
0122-00									0.50	0.12	1
0133+47	2.40	0.12	3.36	0.17	2.93	0.16	2.79	0.43	2.31	0.25	2
0146+05									0.43	0.11	6
0147+18									0.25	0.15	6
0148+27			0.58	0.03	0.48	0.06			0.33	0.11	6
0201+11									-0.14	0.15	6
0202+14			3.26	0.16	1.87	0.11			0.91	0.14	6
0202+31			1.34	0.07	0.73	0.07			0.21	0.15	6
0218+35			1.04	0.05	0.74	0.07			0.40	0.15	1
0219+428									-0.01	0.15	12
0221+06			0.68	0.04	0.81	0.07			1.02	0.18	9
0224+67			1.11	0.06	1.06	0.08	1.29	0.22	1.19	0.19	13
0229+13	1.28	0.07	1.59	0.08	2.02	0.12	2.56	0.40	1.54	0.21	4
0234+28	1.19	0.06	3.34	0.17	3.33	0.18	3.40	0.52	2.03	0.25	9
0235+16	2.61	0.13	3.01	0.15	2.45	0.14	2.26	0.35	2.20	0.26	6
0237-02	0.36	0.03	0.66	0.03	1.17	0.08	1.18	0.20	1.47	0.21	10
0237+04									0.43	0.16	13
0239+10			0.90	0.05	0.82	0.07			0.92	0.17	6
0248+43									0.09	0.15	3
0250+17									0.15	0.15	6
0256+07									0.45	0.11	6
0300+47	1.73	0.09	2.22	0.11	3.07	0.16	3.33	0.51	2.21	0.24	8
0306+10	0.42	0.03	0.70	0.04	1.30	0.08	1.75	0.28	1.84	0.23	6
0309+41			0.40	0.02	0.58	0.07			0.66	0.16	3
0316+41	10.36	0.52	44.90	2.25	43.39	2.17	43.43	6.52	30.50	3.00	1
0317+18									0.15	0.15	6
0332+07									-0.01	0.15	6
0336-01	1.89	0.10	2.43	0.12	2.12	0.12	2.05	0.32	1.63	0.22	1
0345+45									0.36	0.11	3

TABLE III. (continued)

SOURCE	1.379 GHZ		4.585 GHZ		15.064 GHZ		22.185 GHZ		90.000 GHZ		
	S±ΔS		S±ΔS		S±ΔS		S±ΔS		S±ΔS		REF
0355+50	4.98	0.25	8.53	0.43	13.64	0.68	15.21	2.28	8.79	0.85	13
0400+25			1.43	0.07	0.83	0.07			0.39	0.11	6
0406+12			1.02	0.05	0.70	0.07			0.88	0.17	1
0420-01	1.05	0.06	1.68	0.08	2.69	0.15	3.32	0.51	4.13	0.41	1
0421+01									0.02	0.15	11
0422+00	1.22	0.06	0.99	0.05	1.24	0.09	1.55	0.25	1.68	0.22	10
0428+20			2.44	0.12	0.92	0.08			0.23	0.15	1
0430+05	6.16	0.31	6.85	0.34	6.14	0.31	5.68	0.86	4.42	0.44	1
0440-00			1.82	0.09	0.95	0.08			0.70	0.16	14
0444+63									0.11	0.15	3
0446+11									0.32	0.15	1
0457+02									0.24	0.15	13
0459+06									0.41	0.16	11
0500+01									0.26	0.15	10
0532+50									0.13	0.15	3
0537+53									0.22	0.15	4
0602+67									0.51	0.12	2
0611+48									0.25	0.15	2
0620+38									-0.20	0.15	3
0630+49									0.21	0.15	2
0636+68									0.13	0.15	4
0646+60									-0.03	0.15	4
0650+37									0.03	0.15	3
0707+47	1.03	0.06	0.94	0.05	0.93	0.08			0.69	0.13	4
0710+43									0.11	0.15	8
0714+45									0.35	0.11	2
0723-00	2.42	0.12	1.94	0.10	1.48	0.09	1.52	0.25	1.35	0.20	10
0727+40									-0.03	0.15	2
0731+47									0.10	0.15	4
0733+30									0.07	0.15	6
0733+59									0.16	0.15	2
0735+17	1.85	0.09	1.96	0.10	1.75	0.11	2.15	0.34	1.96	0.24	1
0736+01	2.50	0.13	2.06	0.10	2.22	0.13	2.64	0.41	3.39	0.36	10
0738+31			1.84	0.09	1.00	0.08			0.48	0.12	6
0743-00									0.39	0.15	10
0743+25									0.19	0.15	3
0745+24	0.51	0.03	0.76	0.04	0.82	0.07			0.80	0.17	4
0746+48									0.33	0.15	4
0748+33			0.63	0.03	0.22	0.06			0.03	0.15	6
0749+54	0.41	0.03	0.37	0.02	0.52	0.07			0.44	0.09	3
0759+18									-0.01	0.15	1
0802+21	1.07	0.06	0.73	0.04	0.28	0.06			0.39	0.15	1
0804+49									0.47	0.12	4
0805+26									0.16	0.15	3
0805+41									0.11	0.15	4
0812+36									0.34	0.11	4
0814+42	1.41	0.07	1.55	0.08	1.46	0.09	1.35	0.23	1.21	0.19	4
0820+22									0.59	0.16	1
0820+56									0.30	0.11	4
0821+39									0.53	0.16	2

TABLE III. (continued)

SOURCE	1.379 GHZ		4.585 GHZ		15.064 GHZ		22.185 GHZ		90.000 GHZ		
	S±ΔS		S±ΔS		S±ΔS		S±ΔS		S±ΔS		REF
0827+24	0.61	0.03	1.07	0.05	1.59	0.09	1.81	0.29	1.33	0.20	1
0828+49	0.94	0.05	1.43	0.07	1.41	0.09	1.60	0.26	1.24	0.19	4
0829+04									0.46	0.16	10
0831+55									0.23	0.15	8
0833+58									0.40	0.11	4
0834+25			0.61	0.03	0.43	0.06			0.30	0.15	1
0839+18									0.30	0.15	1
0849+28									0.19	0.15	6
0850+58									0.32	0.15	4
0851+20	1.46	0.07	1.74	0.09	2.02	0.11	2.80	0.43	2.64	0.29	1
0859+47									0.37	0.15	4
0900+42									0.23	0.15	2
0900+52									0.04	0.15	2
0906+01	0.84	0.05	0.68	0.04	1.08	0.08			1.01	0.18	10
0913+39									0.29	0.15	4
0917+44			0.75	0.04	1.26	0.09			0.89	0.17	4
0917+62									0.54	0.16	4
0922+00									0.22	0.15	10
0922+40									0.40	0.15	2
0923+39	2.29	0.12	7.21	0.36	7.95	0.40	6.17	0.93	2.93	0.32	4
0941+52									0.02	0.15	4
0945+40									0.05	0.15	4
0953+25	0.86	0.05	1.86	0.09	1.62	0.09	1.93	0.31	1.36	0.20	1
0954+65									0.42	0.16	4
0955+47	0.58	0.04	0.95	0.05	1.36	0.09			0.70	0.16	4
1010+35									0.19	0.15	1
1011+25	0.52	0.03	0.67	0.03	0.89	0.07			-0.01	0.15	1
1013+20			0.77	0.04	0.46	0.06			0.16	0.15	1
1015+35									0.46	0.16	4
1019+30									0.20	0.15	2
1019+42									0.01	0.15	2
1020+40									0.10	0.15	2
1030+39									-0.03	0.15	4
1030+41									0.57	0.16	4
1030+61									0.23	0.11	8
1033+22	0.33	0.03	0.36	0.02	0.31	0.06			0.41	0.16	1
1038+52									0.23	0.15	2
1049+21	1.08	0.06	0.99	0.05	1.02	0.08			0.82	0.17	1
1055+01	2.71	0.14	2.94	0.15	2.65	0.14	2.84	0.44	1.86	0.23	10
1058+39									-0.05	0.15	2
1059+28			0.46	0.02	0.41	0.06			0.52	0.16	1
1101+38	0.63	0.03	0.61	0.03	0.64	0.05	0.44	0.12	0.54	0.12	2
1109+35									-0.11	0.15	2
1111+14									0.24	0.15	1
1119+18									0.13	0.15	1
1123+26	0.78	0.04	1.20	0.06	0.92	0.08			0.52	0.16	1
1128+38									0.50	0.16	2
1144+40			1.29	0.07	1.78	0.11	1.89	0.30	1.36	0.20	2
1144+54									0.23	0.15	4
1146+59									-0.14	0.15	2

1978AJ.....83..685O

TABLE III. (continued)

SOURCE	1.379 GHZ		4.585 GHZ		15.064 GHZ		22.185 GHZ		90.000 GHZ		
	S±ΔS		S±ΔS		S±ΔS		S±ΔS		S±ΔS		REF
1147+24			0.87	0.04	0.80	0.07			0.50	0.16	1
1148-00	3.06	0.15	1.84	0.09	1.47	0.09	1.64	0.27	0.87	0.17	10
1155+25			0.89	0.05	0.39	0.06			-0.22	0.15	1
1155+48									0.14	0.15	2
1214+58									-0.06	0.15	2
1216+48									0.44	0.16	4
1219+04	0.72	0.04	0.72	0.04	0.91	0.08	1.34	0.22	1.09	0.18	10
1219+28	1.43	0.07	1.37	0.07	0.98	0.08	1.15	0.20	0.96	0.18	1
1226+02	41.50	2.08	41.15	2.06	34.63	1.73	32.37	4.86	20.28	1.96	10
1227+25									0.28	0.15	3
1240+38									0.13	0.15	2
1250+53									-0.03	0.15	2
1300+58									0.44	0.16	4
1307+56									-0.21	0.15	2
1308+32	1.04	0.05	1.86	0.09	2.95	0.15	2.98	0.46	2.74	0.27	9
1312+53									0.08	0.15	2
1314+20			0.30	0.02	0.14	0.06			0.37	0.15	1
1327+50									0.24	0.15	2
1333+45									0.10	0.15	4
1333+58									-0.07	0.15	2
1335+55									0.30	0.15	4
1342+663									0.12	0.15	4
1342+662									0.48	0.16	7
1343+45									0.15	0.15	3
1347+53									-0.03	0.15	4
1349+64									0.00	0.15	5
1404+28			2.94	0.15	1.63	0.10			0.36	0.09	13
1415+46									0.16	0.15	4
1418+54	0.61	0.04	0.73	0.04	0.76	0.07	0.74	0.15	0.70	0.16	4
1434+23			0.59	0.03	0.67	0.07			0.58	0.12	1
1436+44									0.02	0.15	2
1441+25									-0.09	0.15	1
1444+17	0.68	0.04	1.10	0.06	0.95	0.08	1.03	0.18	0.63	0.16	1
1456+04	0.22	0.02	0.51	0.03	0.87	0.07	0.86	0.16	1.07	0.18	10
1459+48	0.40	0.03	0.49	0.03	0.48	0.06	0.39	0.12	0.68	0.16	4
1502+10	2.05	0.10	2.47	0.12	2.07	0.12	2.04	0.32	1.42	0.20	1
1504+37	1.10	0.06	1.17	0.06	1.01	0.08	0.94	0.17	0.87	0.17	2
1526+67									-0.06	0.15	4
1532+01	1.10	0.06	0.98	0.05	0.69	0.07	0.60	0.13	0.65	0.16	10
1535+00									0.16	0.15	10
1538+14									0.52	0.16	1
1546+02	0.84	0.05	0.90	0.05	0.82	0.07	0.94	0.17	1.04	0.18	10
1547+50									0.31	0.15	2
1551+13									-0.01	0.15	1
1555+00	1.68	0.09	2.58	0.13	2.42	0.13	2.44	0.38	1.39	0.20	10
1600+33			2.08	0.10	0.99	0.08			0.55	0.16	6
1604+31			0.60	0.03	0.23	0.06			0.01	0.15	6
1607+26			1.86	0.09	0.43	0.06			0.21	0.15	1
1611+34			2.36	0.12	1.68	0.10	1.44	0.24	0.86	0.17	6
1624+41									0.39	0.15	8

TABLE III. (continued)

SOURCE	1.379 GHZ		4.585 GHZ		15.064 GHZ		22.185 GHZ		90.000 GHZ		
	S±ΔS		S±ΔS		S±ΔS		S±ΔS		S±ΔS		REF
1633+38	1.49	0.08	1.79	0.09	1.65	0.10	1.73	0.28	1.08	0.18	4
1636+47									0.10	0.11	2
1637+57	0.79	0.04	1.31	0.07	1.12	0.08	1.30	0.22	0.79	0.17	4
1638+39									0.21	0.15	2
1641+39	7.28	0.36	7.78	0.39	8.41	0.42	9.02	1.36	6.15	0.61	4
1642+69	0.99	0.05	1.11	0.06	2.45	0.14	3.16	0.48	2.84	0.31	4
1652+39			1.26	0.06	0.95	0.08	0.90	0.17	0.69	0.16	1
1656+34									0.24	0.15	4
1656+47									0.60	0.16	4
1656+48									0.55	0.16	2
1656+57									0.20	0.15	2
1714+21			0.52	0.03	0.40	0.06			0.37	0.15	6
1716+68	0.42	0.03	0.61	0.03	1.04	0.08	1.03	0.18	0.67	0.16	4
1719+35			0.82	0.04	0.78	0.07	0.74	0.15	0.64	0.16	2
1722+40									0.08	0.15	4
1726+45			1.09	0.06	0.94	0.08	1.08	0.19	0.77	0.17	4
1734+50									0.09	0.15	4
1738+49									0.33	0.15	4
1751+28			0.94	0.05	0.79	0.07			0.55	0.16	6
1807+27			0.50	0.03	0.25	0.06			0.26	0.15	6
1807+69	1.72	0.09	1.90	0.10	2.20	0.13	2.13	0.33	1.37	0.20	4
1823+56	1.14	0.06	1.54	0.08	1.82	0.11	1.88	0.30	1.44	0.20	4
1842+68			1.09	0.06	1.22	0.09			0.65	0.16	5
1848+28			0.80	0.04	0.66	0.07			0.29	0.15	6
1926+61									0.14	0.15	3
1954+51			1.34	0.07	1.26	0.09	1.44	0.24	0.69	0.16	2
2021+61									0.20	0.15	2
2200+42			4.81	0.24	4.82	0.25			3.95	0.41	4
2214+35					0.52	0.07			0.10	0.15	1
2228+69									0.05	0.15	8
2253+41									0.35	0.15	2
2319+27			0.90	0.05	0.72	0.07			0.35	0.15	12
2323+42									0.39	0.15	7
2337+26			0.83	0.04	0.31	0.06			-0.19	0.15	12
2346+38									0.26	0.15	4
2351+45									-0.13	0.15	2
2357+38			0.58	0.03	0.48	0.06			0.00	0.15	4

Notes to TABLE III

1. Adgie (1974)
2. Bonn 100 m (in Green Bank survey papers Pauliny-Toth *et al.* 1972, 1978, Pauliny-Toth and Kellermann, 1972)
3. Table IV (this paper)
4. Green Bank interferometer (in Green Bank survey papers)
5. Cal Tech interferometer 21 cm (in Green Bank survey papers)
6. Cal Tech interferometer 6 cm (in Green Bank survey papers)
7. 91 m Green Bank (in Green Bank survey papers)
8. Cohen *et al.* (1977)
9. Ghigo and Owen (1973)
10. Brandie and Bridle (1974)
11. McEwan *et al.* (1975)
12. Owen and Rudnick (1976)
13. Green Bank interferometer calibrator list
14. Sharp and Bash (1975)

vation is 150 mJy and thus 3σ detections can only be claimed for $S_{90} > 0.45$ Jy. However, the distribution of observed flux densities below 0.45 Jy is clearly skewed away from 0 and has a positive mean of 0.17 Jy. This mean is significantly different from zero (at much better than 1% significance level) and suggests that most of the sources with observed flux densities below the 3σ limit must typically have small positive flux densities $\gtrsim 0.1$ Jy. This result is consistent with a model in which most of these non-detections are sources which become opti-

TABLE IV. Positions for sources measured with the Green Bank interferometer.

Source	R. A. (1950.0)	Dec (1950.0)
0248 + 43	02 48 18.47	43 02 57.1
0309 + 41	03 09 44.76	41 08 49.0
0345 + 45	03 45 46.86	46 00 52.3
0444 + 63	04 44 42.33	63 26 55.9
0532 + 50	05 32 25.59	50 36 34.6
0620 + 38	06 20 51.49	38 58 27.7
0650 + 37	06 50 35.26	37 09 27.6
0743 + 25	07 43 23.03	25 56 25.4
0749 + 54	07 49 06.43	54 00 46.4
0805 + 26	08 05 34.24	26 55.24.7
1019 + 30	10 19 39.87	30 56 15.5
1227 + 25	12 27 44.33	25 34 41.4
1343 + 45	13 43 28.83	45 07 59.5

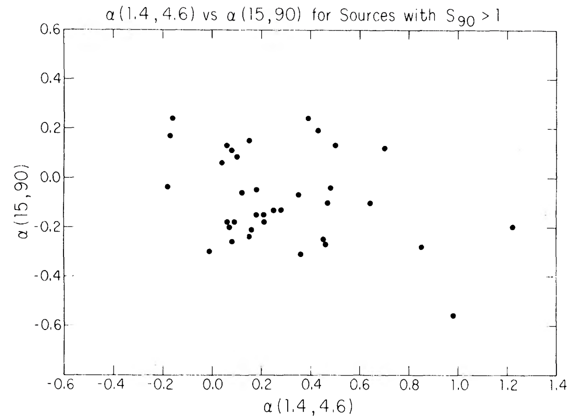

FIG. 3. $\alpha(1.4, 4.6)$ vs $\alpha(15, 90)$ for all sources with $S_{90} > 1$ which have flux densities measured at all four frequencies.

cally thin at frequencies $\sim$10 GHz and thereafter have spectral indices ~ -0.8 as is typical of spectral flux distributions for sources detected at lower frequencies. However, other spectral flux distributions are also possible.

b) Radio Spectra

The most striking result shown by the radio spectra in Fig. 1 is the tendency of the sources to have flat radio spectra over the range of 1–100 GHz. The radio color-color diagram, $\alpha(1.4, 4.6)$ vs $\alpha(15, 90)$, for sources with $S_{90} > 1$ (Fig. 3) emphasizes this result. With a few exceptions all the sources fall in the region $0.5 > \alpha(1.4, 4.6) > -0.2$ and $0.3 > \alpha(15, 90) > -0.3$. Thus the sample may show some tendency to have steeper, positive spectral indices at the low frequency end but seems to scatter about $\alpha(15, 90) \sim -0.1$ at the higher frequency end of the color plot. Thus a flat radio spectrum seems to be a general characteristic of sources with $S_{90} > 1$ Jy at least those selected in the manner of our sample.

In Fig. 4, we compare the spectral properties of the sources with $S_{90} > 1$ Jy with those from Paper I with $S_{90} < 0.5$ Jy. As might be expected, the weaker sources in our sample at 90 GHz have spectra which tend to turn over at/or near 5 GHz. Thus the strong millimeter sources have spectra which are significantly different from most sources found to have flat or inverted spectra at lower frequencies. It thus would not be surprising if their properties at other, higher frequencies were significantly different.

In Fig. 5 we show a histogram of m_E (the rough visible magnitude estimated from the sky survey E-print) from Paper I for three ranges of $\alpha(4.6, 15)$. A tendency can be seen for sources with larger values of α (i.e., those which turnover at higher frequencies) to be brighter optically. This result is in agreement with the trends reported by Usher (1975) for sources with spectra obtained from nonsimultaneous measurements and suggests some relation between the radio and optical emission processes. It also is in agreement with our results from Paper I.

Since at least eight of these sources have continuous optical spectra, we agree with the result of Pacht (1976) that BL Lac objects tend to have flat spectra. However, the flatness of the radio spectra could just as well be due to a correlation between millimeter activity and a continuous optical spectrum, since most strong millimeter sources have flat spectra.

c) Variability at 90 GHz

While the variability of radio sources at millimeter wavelengths is well established (e.g., Hobbs and Dent

TABLE V. Optical observations.

Source	UT Date	V	$(B-V)$	$(U-B)$	830 THz (U) (mJy)	680 THz (B) (mJy)	540 THz (V) (mJy)	Number of observations
0814 + 42	15 Jan 77	18.18 ± .08	0.70 ± .11	−0.36 ± .13	0.07	0.12	0.20	1
0827 + 24	15 Jan 77	17.26 ± .03	0.36 ± .04	−0.79 ± .03	0.35	0.40	0.48	1
0828 + 49	15 Jan 77	18.82 ± .14	0.64 ± .19	−0.61 ± .19	0.05	0.07	0.11	1
0851 + 20	15 Jan 77	15.43 ± .02	0.48 ± .02	−0.51 ± .02	1.30	1.92	2.56	3
0953 + 25	15 Jan 77	17.90 ± .04	0.08 ± .05	−0.50 ± .04	0.19	0.29	0.26	1
1219 + 28	16 Jan 77	16.11 ± .05	0.70 ± .04	−0.52 ± .04	0.57	0.83	1.37	1
1308 + 32	15 Jan 77	14.45 ± .01	0.37 ± .02	−0.57 ± .02	3.75	5.24	6.32	4
	16 Jan 77	14.43 ± .02	0.36 ± .02	−0.56 ± .02	3.82	5.39	6.44	10
	18 Jan 77	14.16 ± .01	0.43 ± .02	−0.54 ± .03	4.51	6.48	8.26	6
1418 + 54	16 Jan 77	15.65 ± .05	0.52 ± .04	−0.44 ± .04	0.96	1.51	2.09	1
1502 + 10	16 Jan 77	18.56 ± .15	0.41 ± .16	−0.51 ± .16	0.08	0.11	0.14	1

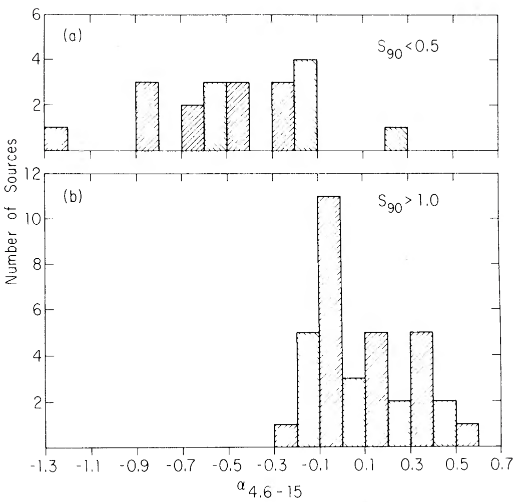

FIG. 4. Histogram of $\alpha(4.6, 15)$ for (a) sources from Paper I with $S_{90} < 0.5$; (b) sources with $S_{90} > 1$.

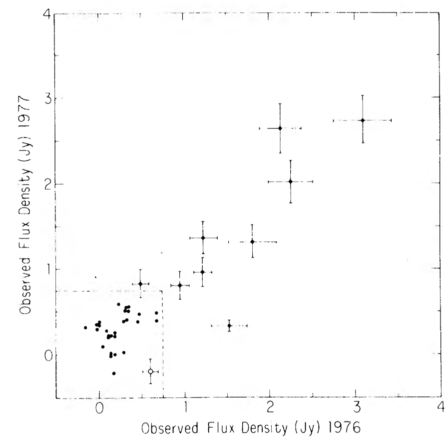

FIG. 6. Flux densities in 1976 versus flux densities in 1977 at 90 GHz for sources from Paper I. Sources stronger than 0.75 Jy at either epoch are shown with individual error bars. Sources weakers than 0.75 Jy at both epochs are shown as dots (inside the dashed box). A characteristic error bar for the sources weaker than 0.75 Jy is also shown inside the dashed box.

1977) most of the sources we observed in 1976 did not vary greatly. In Fig. 6, we have plotted the flux densities measured in 1976 versus those measured in 1977. For sources weaker than 0.75 Jy by both epochs (those sources inside the dashed box), the measurements are represented by a dot and a characteristic error bar is given for all the points. For sources stronger than 0.75 Jy at either epoch, the individual error bars are shown. It is apparent that very few of the sources have varied significantly over the one year time scale. In particular, none of the weak sources have made a dramatic rise out of the noise. In addition, most of the strong sources are consistent with a variability of less than 30% for one year.

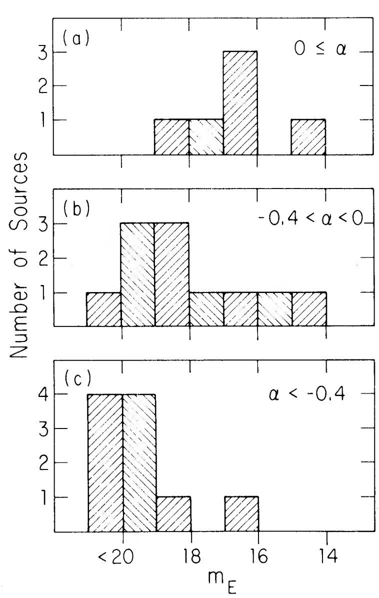

FIG. 5. Histogram of m_E (from Paper I) for (a) $\alpha(4.6, 15) > 0$ (b) $-0.4 < \alpha(4.6, 15) < 0$ (c) $\alpha(4.6, 15) < -0.4$.

Only one source varied radically; 0109 + 22 decreased by a factor of 4.5 between the two epochs. Thus, while variability at millimeter wavelengths can be rapid (e.g., A0235 + 164; Rieke *et al.* 1976) such changes are relatively rare.

IV. DISCUSSION

The generally flat radio spectra which we observe for most strong millimeter sources in our sample present serious problems for incoherent models involving one or two simple homogeneous components to explain all the radio emission. Many of these sources probably consist of two components at centimeter wavelengths (e.g., 3C 120, 3C 273B; Schilizzi *et al.* 1975, 3C 345; Cohen *et al.* 1976, Wittles *et al.* 1976). However, little is known about the spectra of the individual components over a significant range in frequency. Comparison of our spectra with that expected for a simple homogeneous source (e.g., Burbidge *et al.* 1974) gives the impression that it would take quite special circumstances to produce a flat spectrum from only a few such components. Numerical experiments (T. Jones, private communication) confirm this impression. Flat spectra produced by homogeneous components would be the rare exception rather than the rule.

An inhomogeneous model with a radial dependence of the magnetic field and relativistic electron densities provides a much better fit to the data (Condon and Dressel 1973, de Bruyn 1976, Marscher 1977a). Marscher (1977b) has emphasized that this point for one source (0735 + 17) and his comments can be generally extended to most of the sources in our sample with $S_{90} > 1$ Jy. It thus seems likely to us that one or more components with inhomogeneous structure probably exist in most of our strong millimeter sources.

The lack of strong variability in most of the sources in Paper I over a timescale of a year may suggest that many of them are relatively large ($\gtrsim 1$ pc). This is consistent with the 10^{12} K brightness temperature limit expected from Compton cooling and found to hold for most of the sources with known redshifts. The more rapid variability seen in a few sources may be explained either by these sources being less distant or by relativistic motions in the line of sight.

Optically the sources appear to be much more variable, indicating that a smaller size than that of the centimeter or millimeter region is likely. For example, 1308 + 32 did not appear to vary by more than 10% over the year in the radio while in the optical it had varied by a factor of ten in a year and by 30% over four days on which we observed it. The optical emission might originate in the inner part of an inhomogeneous source where the magnetic field and relativistic particle densities have stopped increasing rapidly allowing the source to become optically thin.

Several of these sources observed in the optical and infrared during this program (O'Dell *et al.* 1978) seem to have power law spectra in these frequency ranges which could be plausibly extrapolated to the optically thick radio region. Thus the optical and infrared spectra are generally consistent with the inhomogeneous picture with a radially decreasing density and/or field distribution.

We would like to express our appreciation to Ms. Marian L. Frueh for producing many of the finding charts used in this project. We also thank S. Spangler for critically reading the manuscript. This work was partly supported by a Grant from the Research Corporation (TJM), which is gratefully acknowledged.

REFERENCES

Adgie, R. L. (1974). Astron. J. **79,** 846.
Brandie, G. W., and Bridle, A. H. (1974). Astron. J. **79,** 903.
Burbidge, G. R., Jones, T. W., and O'Dell, S. L. (1974). Astrophys. J. **193,** 43.
Cohen, A. M., Porcas, R. W., Browne, I. W. A., Daintree, E. J., and Walsh, D. (1977). Men. R. Astron. Soc. **84,** 1.
Cohen, M. H., Moffet, A. T., Romney, J. D., Schilizzi, R. T., Seielstad, G. A., Kellermann, K. I., Purcell, G. H., Shaffer, D. B., Pauliny-Toth, I. I. K., Preuss, E., Witzel, A., and Rinehart, R. (1976). Astrophys. J. Lett. **206,** L1.
Condon, J. J., and Dressel, L. L. (1973). Astrophys. Lett. **15,** 203.
Condon, J. J., and Jauncey, D. L. (1974). Astron. J. **79,** 1220.
de Bruyn, A. G. (1976). Astron. Astrophys. **52,** 439.
Genzel, R., Pauliny-Toth, I. I. K., Preuss, E., and Witzel, A. (1976). Astron. J. **81,** 1084.
Ghigo, F. D., and Owen, F. N. (1973). Astron. J. **79,** 1220.
Heeschen, D. S. (1975). Sky and Telescope **49,** 344.
Hobbs, R. W., and Dent. W. A. (1977). Astron. J. **82,** 257.
Kellermann, K. I., Pauliny-Toth, I. I. K., and Williams, R. J. S. (1969). Astrophys. J. **157,** 1.
Kellermann, K. I., and Pauliny-Toth, I. I. K. (1973). Astron. J. **78,** 828.
Kitt Peak User's Manual (1977). Kitt Peak Publication.
Landolt, A. U. (1973). Astron. J. **78,** 959.
Liller, W. (1976). IAU Circ. No. 2939.
Marscher, A. P. (1977a). Astrophys. J. **216,** 244.
Marscher, A. P. (1977b). Astron. J. **82,** 781.
McEwan, N. J., Browne, I. W. A., and Crowther, J. H. (1975). Mem. R. Astron. Soc. **80,** 1.
O'Dell, S. L., Puschell, J. J., and Stein, W. A. (1977). Astrophys. J. **213,** 351.
O'Dell, S. L., Puschell, J. J., Stein, W. A., Owen, F. N., Porcas, R. W., Mufson, S. L., Moffett, T. J., and Ulrich, M.-H. (1978). Astrophys. J. In press.
Owen, F. N., and Mufson, S. L. (1977). Astron. J. **82,** 776.
Owen, F. N., and Rudnick, L. (1976). Astrophys. J. **203,** 307.
Patch, E. (1976). Astron. J. **81,** 1574.
Pauliny-Toth, I. I. K. and Kellermann, K. I. (1972). Astron. J. **77,** 797.
Pauliny-Toth, I. I. K., Kellermann, K. I., Davis, M. M., Fomalont, E. B., and Shaffer, D. B. (1972). Astron. J. **77,** 265.
Pauliny-Toth, I. I. K., Witzel, A., Preuss, E., Kuhr, H., Kellermann, K. I., Fomalont, E. B., and Davis, M. M. (1978). Astron. J. In press.
Porcas, R. W. (1975). Ph.D. thesis, Univ. Manchester, England.
Rieke, G. H., Grasdalen, G. L., Kinman, T. D., Hintzen, P., Wills, B. J., and Wills, D. (1976). Nature **260,** 751.
Schilizzi, R. T., Cohen, M. H., Romney, J. D., Shaffer, D. B., Kellermann, K. I., Swenson, G. W., Jr., Yen, J. L., and Rinehart, R. (1975). Astrophys. J. **201,** 263.
Sharp, J. R., and Bash, F. N. (1975). Astron. J. **80,** 335.
Tapia, S., Craine, E. R., and Johnson, K. (1976). Astrophys. J. **203,** 291.
Ulrich, M. H., and Owen, F. N. (1977). Nature **269,** 673.
Usher, P. D. (1975). Astrophys. J. **198,** L53.
VLA User Manual (1977). NRAO publication.
Wall, J. V., Shimmins, A. J., and Merkelin, J. K. (1971). Aust. J. Phys. Astrophys. Suppl. **19,** 1.
Wittels, J. O., Cotton, W. D., Counselman, C. C. III, Shapiro, I. I., Hinteregger, G. F., Knight, C. A., Rogers, A. E. E., Whitney, A. R., Clark, T. A., Hutton, L. K., Ronnang, B. O., Rydbeck, O. E. H., and Niell, A. E. (1976). Astrophys. J. (Lett.) **206,** L75.